1987AJ.....94.1350W

THE ASTRONOMICAL JOURNAL VOLUME 94, NUMBER 5 NOVEMBER 1987

ROTATIONAL DYNAMICS OF IRREGULARLY SHAPED NATURAL SATELLITES

JACK WISDOM
Department of Earth, Atmospheric, and Planetary Sciences, Massachusetts Institute of Technology, Cambridge, Massachusetts 02139
Received 23 February 1987; revised 21 July 1987

ABSTRACT

All irregularly shaped natural satellites must tumble chaotically before being captured into synchronous rotation.

I. INTRODUCTION

The basic mechanisms governing the tidal evolution of the obliquities and rotation rates of the natural satellites have been understood for over 100 yr (Darwin 1879; see Goldreich and Peale 1970). If the spin angular velocity is large, the tidal torque tends to drive the obliquity to an equilibrium value between 0° and 90°. As the spin is slowed by tidal friction, the equilibrium obliquity decreases. If the orbit is fixed, the equilibrium obliquity goes to zero as the spin angular velocity approaches twice the mean orbital motion. For smaller angular velocities, the equilibrium obliquity is zero. Until the discovery of the resonant rotation of Mercury (Pettengill and Dyce 1965), the rate of rotation was assumed to decline steadily until the synchronous lock was established. The resonant rotation of Mercury forced a reevaluation of this picture, and the theory of spin-orbit coupling was developed (see Goldreich and Peale 1966). For a fixed orbit with nonzero eccentricity and a figure that is not too out-of-round, spin-orbit resonances with rotation rates equal to half an integer multiple of the orbital mean motion were shown to be dynamically stable, and in many cases motion in these resonances is stable against further tidal evolution as well. The probability of capture into each of these nonsynchronous spin-orbit resonances as it is encountered was estimated. However, Peale (1977) has shown that, among those natural satellites for which the timescale for despinning is smaller than the age of the solar system, none has a significant probability of having been captured into a nonsynchronous commensurate spin-orbit resonance. In those cases where the rotation state is known, all tidally evolved satellites are in synchronous rotation. It is rather unfortunate that the only example of a nonsynchronous commensurate rotation in the solar system is the one that inspired this elegant theory.

Saturn's satellite Hyperion is a dramatic exception to this general picture (Wisdom, Peale, and Mignard 1984). The rotation of Hyperion has been significantly affected by tidal friction and consequently the rotation rate is expected to be comparable to the orbital mean motion (Peale 1977). *Voyager* pictures showed Hyperion to be significantly out-of-round, with the long axis roughly twice as long as the short axis (Smith *et al.* 1982). The standard theory of spin-orbit coupling is not valid for a body with such large asphericity. A reanalysis of the spin-orbit problem using techniques of modern nonlinear dynamics showed that in fact for Hyperion the rotational phase space near synchronous rotation is dominated by a large chaotic zone. The chaotic zone extends from no rotation at all in an inertial frame to nearly two and a half revolutions per orbit. This region is so strongly perturbed that the 3/2 resonance, the resonance in which the rotation of Mercury is locked, is not stable. Even more interesting, the synchronous spin-orbit resonance, in which all other tidally evolved natural satellites are found, is attitude unstable. Even if Hyperion were placed in synchronous rotation with the spin axis perpendicular to the orbital plane, under the slightest perturbation the spin axis would fall away from the orbit normal and Hyperion would begin to tumble. Moreover, the chaotic zone is also attitude unstable. As Hyperion's rotation was slowed by tidal friction, there came a point when it entered the chaotic zone with its spin axis nearly perpendicular to the orbit plane. Since this axis orientation is unstable, Hyperion then began to tumble. The calculation of the Lyapunov Characteristic Exponents (LCEs) shows that the tumbling motion is fully chaotic. Two spin-orbit resonances are accessible to Hyperion from this chaotic-tumbling state that are attitude stable: the 2/1 resonance and the second-order 9/4 resonance. Ultimately, Hyperion must be captured by one of these resonances, but all observations to date are consistent with Hyperion currently being in the chaotic-tumbling state (Goguen 1983; Thomas *et al.* 1984; Thomas and Veverka 1985; Binzel *et al.* 1986). Perhaps the most convincing evidence for the chaotic tumbling of Hyperion is the large angle of the long axis from the orbit plane.

The presence of the large chaotic zone can be understood in terms of the resonance-overlap criterion (see Wisdom *et al.* 1984). A large chaotic zone is expected whenever the sum of the widths of the libration zones for neighboring resonances computed individually is larger than the separation between the resonances. For the spin-orbit problem, the widths of the resonances are all proportional to the asphericity parameter $\alpha = \sqrt{3(B-A)/C}$, where $A < B < C$ are the principal moments of inertia. In addition, the widths of all of the resonances except for the synchronous resonance are proportional to some power of the eccentricity. Hyperion is not only out-of-round ($\alpha \approx 0.89$), but the orbit of Hyperion has a rather large eccentricity, near 0.1. This eccentricity is primarily a forced eccentricity due to the 4/3 mean motion commensurability between Titan and Hyperion. An asphericity parameter of order unity and large orbital eccentricity gives a strong overlap of primary resonances, and thus accounts for the large chaotic zone in Hyperion's rotational phase space. Should other natural satellites be expected to be chaotically tumbling? There are actually a number of other natural satellites that are significantly out-of-round, but in each case the orbital eccentricity is low. In those cases where the rotation is known, these satellites are all in synchronous rotation; the synchronous resonance is attitude stable. With its large orbital eccentricity ($e \approx 0.75$) and size comparable to that of Hyperion, Nereid comes to mind as a possible candidate for chaotic tumbling, but in this case there is no

 0004-6256/87/051350-11$00.90 © 1987 Am. Astron. Soc. 1350

© American Astronomical Society • Provided by the NASA Astrophysics Data System

1987AJ.....94.1350W

reason to believe that Nereid is tidally evolved to a near synchronous rotation (Peale 1977). The rotation of Nereid is most likely spin stabilized. Like the classical spin-orbit theory from which it was developed, the theory of Hyperion's chaotic rotation apparently has only a single follower today.

It may be the case though that other natural satellites rotate chaotically at some point in their rotation histories. In fact, since all spin-orbit resonances are surrounded by chaotic separatrices (see Wisdom *et al.* 1984; Chirikov 1979), it is certain that all satellites that were captured into synchronous rotation from nonsynchronous rotation crossed a chaotic separatrix. In many cases, this chaotic separatrix is exponentially small and would have had no significant effect on the evolution. For example, the width of the separatrix surrounding the 3/2 resonance of Mercury may be estimated to be of order 10^{-43} times the width of the 3/2 resonance (Wisdom *et al.* 1984). Tidal friction pulls Mercury across the chaotic separatrix in a single libration period. In other cases, the chaotic separatrices are not so microscopic. The estimate of the width of the chaotic separatrix for the synchronous spin-orbit resonance given in Wisdom *et al.* (1984) (see also Eq. (4) below) depends exponentially on the out-of-roundness parameter α, but only linearly on the orbital eccentricity. Thus satellites that are significantly out-of-round may be expected to have chaotic separatrices of significant size even if the orbital eccentricity is relatively small. For several of the irregularly shaped satellites the chaotic separatrix engulfs both the 3/2 and the 1/2 resonances (Sec. II). A more surprising result is that in every case the chaotic zone is attitude unstable, and the resulting chaotic-tumbling motion carries the long axis of the satellite through a significant angle from the orbital plane (Sec. III). The magnitude of this deflection seems to be relatively insensitive to the orbital eccentricity. Even for Deimos, where the orbital eccentricity is anomalously low ($e \approx 0.0005$), the angle from the long axis to the orbital plane gets as large as 0.86 rad. This result suggests that the out-of-plane tumbling motion would occur even for circular orbits. Reducing the problem even further, it turns out that even a prolate axisymmetric body in a circular orbit can be attitude unstable to chaotic tumbling at the point of entry into synchronous rotation. In this case the motion is reducible to a two degree of freedom problem and surfaces of section can be computed that display the geometry of the phase space of the tumbling motion (Sec. IV). It is not possible to enter the synchronous spin-orbit resonance without passing through the attitude-unstable chaotic separatrix. All of the irregularly shaped natural satellites must have spent a certain amount of time in this chaotic-tumbling state. The enhanced dissipation in a tumbling satellite may significantly affect the orbital evolution and must certainly be taken into account in considering the orbital history of an irregular-shaped satellite (Sec. V). This episode of chaotic tumbling may help explain the anomalously low eccentricity of the orbit of Deimos or perhaps the "stretch marks" on Phobos (Sec. VI).

II. SURFACES OF SECTION

In this section the spin-orbit coupling problem with the spin-axis fixed perpendicular to the orbit plane is considered. This problem was reviewed by Wisdom *et al.* (1984). It is natural to consider this reduced problem since in the standard picture of tidal evolution the spin axis is driven perpendicular to the orbit plane. The satellite has principal moments of inertia $A < B < C$, and C is the moment about the spin axis which is fixed perpendicular to the orbit plane. The orbit is taken to be a fixed ellipse with semimajor axis a, eccentricity e, true anomaly f, instantaneous radius r, and longitude of periapse $\tilde{\omega}$, which is taken as the origin of longitudes. The orientation of the satellite's long axis is specified by θ and thus $\theta - f$ measures the orientation of the satellite's long axis relative to the planet-to-satellite line. The equation of motion for θ is

$$\frac{1}{n^2}\frac{d^2\theta}{dt^2} + \frac{\alpha^2}{2}\left(\frac{a}{r}\right)^3 \sin 2(\theta - f) = 0, \tag{1}$$

where n is the orbital mean motion and, again, $\alpha = \sqrt{3(B-A)/C}$. With the spin axis constrained to be perpendicular to the orbit plane, the spin-orbit problem has one degree of freedom with explicit periodic time dependence through the true anomaly and the instantaneous radius.

Most Hamiltonian systems have both regular and irregular trajectories. The phase space is divided; there are regions in which trajectories behave chaotically and regions where trajectories are quasiperiodic. The structure of the phase space of a system with two degrees of freedom or of a nonautonomous (time-dependent) system with one degree of freedom is most easily understood by computing surfaces of section (see Hénon and Heiles 1964). Since the spin-orbit problem depends periodically on the time, the most convenient surface of section is made by plotting the rate of change of the orientation $d\theta/dt$, versus the orientation θ, once per orbit period at periapse. The choice of periapse over other orbital phases is arbitrary. For ease of understanding, the rate of change of the orientation is normalized by the mean motion. On the surface of section, successive points belonging to a quasiperiodic trajectory will appear to be restricted to a curve, while successive points belonging to a chaotic trajectory appear to fill an area. On the spin-orbit surfaces of section, the commensurate spin-orbit resonances appear as islands of quasiperiodic orbits which do not cover all values of θ. (Note that because of the symmetry of the principal axis system, θ and $\theta + \pi$ are dynamically equivalent configurations. Only that portion of the section for θ between 0 and π is plotted.)

For Hyperion, where $\alpha \approx 0.89$ and $e \approx 0.1$, the phase space near synchronous rotation is dominated by a large chaotic zone in which $d\theta/dt$ varies from 0 to $2.5n$. For other irregularly shaped natural satellites in the solar system, the parameter α is the same order of magnitude as that of Hyperion (see Table I), but a crucial difference for the dynamics is that the orbits are not nearly so eccentric. In fact, for zero eccentricity, Eq. (1) is integrable. In this case, $r = a$ and $f = nt$. Changing variables to $\theta' = \theta - nt$, the new equation of motion is

$$\frac{1}{n^2}\frac{d^2\theta'}{dt^2} + \frac{\alpha^2}{2}\sin 2\theta' = 0. \tag{2}$$

Except for the factors of 2, which could easily be removed by a further change of variables, this is the equation of motion for a pendulum for which the solutions may be explicitly written in terms of elliptic functions. This equation of motion has the integral

$$I = \frac{1}{2}\left(\frac{1}{n}\frac{d\theta'}{dt}\right)^2 - \frac{\alpha^2}{4}\cos 2\theta'. \tag{3}$$

It is easily verified that the frequency of small amplitude oscillations is $\omega_0 = \alpha n$. The half-width of the libration region in $d\theta/dt$ is also αn. Evidently, there is no chaotic behavior in the spin-orbit problem with the spin axis fixed perpen-

© American Astronomical Society • Provided by the NASA Astrophysics Data System

1987AJ.....94.1350W

TABLE I. Data for irregularly shaped natural satellites.

Satellite	Shape (km)	α	e	$\Delta\left(\frac{1}{n}\frac{d\theta}{dt}\right)$	$\lvert\phi\rvert_{max}$
Phobos	$(13.5\pm 1)\times(10.5\pm 0.7)\times(9.0\pm 0.7)$	0.86	0.015	0.58	1.29
Deimos	$(7.5\pm{}^{3}_{1})\times(6.0\pm 0.5)\times(5.0\pm 1)$	0.81	0.0005	0.09	0.86
Amalthea	$(135\pm 5)\times(85\pm 5)\times(75\pm 5)$	1.14	0.003	0.16	0.98
Janus	$(110\pm 5)\times(95\pm 5)\times(80\pm 5)$	0.66	0.009	0.34	0.85
Epimetheus	$(70\pm 8)\times(57\pm 8)\times(50\pm 5)$	0.78	0.007	0.30	0.92
1980S26	$(55\pm 8)\times(42\pm 5)\times(33\pm 5)$	0.89	0.004	0.23	0.85
1980S27	$(70\pm 5)\times(50\pm 7)\times(37\pm 8)$	0.99	0.004	0.21	0.94

dicular to the orbit plane unless the eccentricity is nonzero. It is a reasonable expectation then that the size of the chaotic zone will increase with the eccentricity. The increase in the size of the chaotic zone cannot, however, be continuous, since there will be critical values of the eccentricity where a new island is suddenly engulfed by the chaotic zone, or equivalently where the last invariant curve separating the chaotic zones surrounding two neighboring islands disappears. Wisdom *et al.* (1984) have given an estimate of the size of the chaotic separatrix when there is no overlap of primary resonances in terms of the chaotic variations of the integral I. For the synchronous spin-orbit resonance this estimate is

$$(I-I_s)/I_s = (14\pi e/\alpha^3)e^{-\pi/2\alpha}, \qquad (4)$$

where I_s is the value of the integral evaluated on the separating trajectory in the integrable $e=0$ case. (Strictly speaking, I should be the averaged resonance Hamiltonian for the synchronous resonance, but this differs from I only by terms of second order in e.) While the width depends exponentially on the parameter α, it is only linearly dependent on the eccentricity. The formula obeys the requirement that the width of the chaotic zone is zero for zero eccentricity, and verifies the expectation that the width increases as the eccentricity increases. The fact that the width depends linearly on the eccentricity (in this approximation) means that those satellites with large α but small e may still have significant chaotic zones. For the satellites considered here, $\alpha > 0.5$ in every case. Thus the synchronous island even extends beyond the nominal position of the 3/2 resonance. Consequently, the estimate (4) for the width may not be very good. The only reliable way of determining the actual extent of the chaotic zone is to compute a surface of section. Figure 1 shows the surface of section for Phobos, where α, as determined from the shape assuming a uniform density, is 0.86, and the eccentricity is taken to be the current eccentricity of 0.015. While the chaotic zone is much narrower than the chaotic zone for Hyperion, it is still a major feature on the surface of section. Note that a single chaotic zone engulfs the synchronous resonance, the 1/2 resonance (the island just below center), and the 3/2 resonance (the small island in the center of the chaotic zone near $\theta = 0$). The observed amplitude of the forced libration of Phobos is only $0^{\circ}.8 \pm 0.2$ (Duxbury and Callahan 1982). This implies an α of only 0.56. It appears that the shape of Phobos does not accurately represent the mass distribution. However, the surface of section for $\alpha = 0.56$ is very similar to the section in Fig. 1. The chaotic zones are just about the same size, but the 3/2 island is somewhat larger for the smaller α.

The orbital eccentricity is a critical factor in determining the width of the fixed-axis chaotic zone. Unfortunately, there is considerable uncertainty in the orbital history of Phobos; the orbital eccentricity at the time when Phobos was captured into the synchronous resonance is not known. Singer(1968), Lambeck(1979), Mignard(1981), and Cazenave *et al.* (1981) all give large eccentricity ($e > 0.6$) to the orbit of Phobos near the time of its formation or capture. The timescale for the tidal despinning of Phobos is on the order of 10^5 yr (Peale 1977) at its current semimajor axis and at most ten million years at its more distant initial location. Synchronous rotation was reached essentially at the time of formation. If the eccentricity was indeed large at the time of capture into synchronous rotation, then Phobos would certainly have had a period of chaotic tumbling in its history. On the other hand, Yoder (1982) (see also Mignard 1981) points out that a number of resonances must have been crossed which could have increased the eccentricity from a near-zero initial value to values several times larger than the current eccentricity. In this case, the observed eccentricity is explained as a tidal remnant of the eccentricity after the last resonance passage rather than a remnant from the formation epoch. Thus the eccentricity of Phobos may have always been small. The width of the chaotic zone may be characterized by the extent of the chaotic zone in $d\theta/dt$ near the unstable equilibrium ($\theta = \pi/2$ on the surface of section). In Fig. 2, the extent of the chaotic zone for Phobos ($\alpha = 0.86$), as determined from rather limited integrations of 2000 orbit periods each, is plotted versus orbital eccentric-

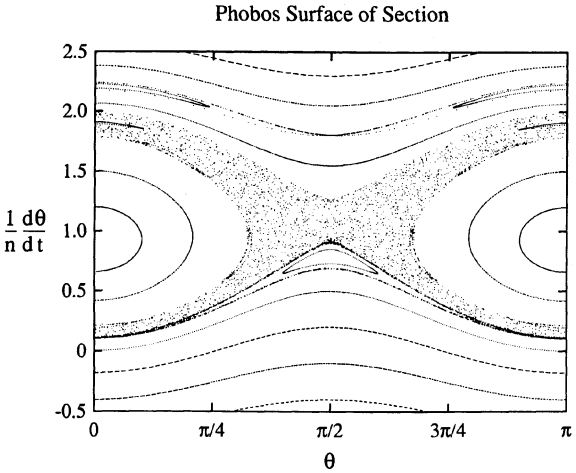

FIG. 1. Surface of section for Phobos with the spin axis constrained to be perpendicular to the orbit plane. The rate of change of the orientation is plotted versus the orientation at every periapse. Here $\alpha = \sqrt{3(B-A)/C} = 0.86$, and the orbital eccentricity is 0.015. The chaotic zone engulfs the 3/2 and 1/2 states as well as the synchronous rotation resonance.

© American Astronomical Society • Provided by the NASA Astrophysics Data System

1987AJ.....94.1350W

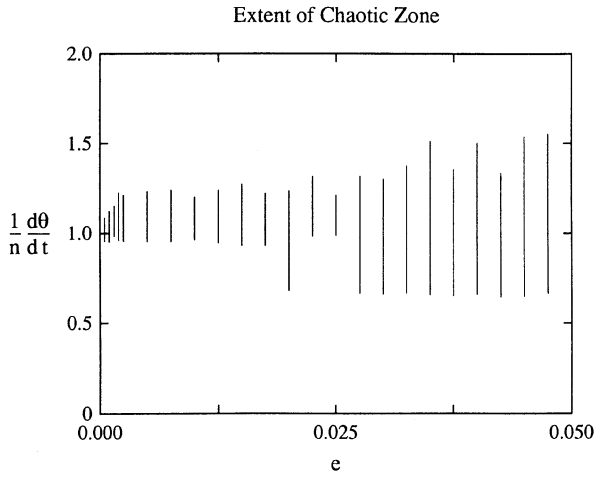

FIG. 2. The extent of the fixed spin-axis chaotic zone at $\theta = \pi/2$ with the figure of Phobos, but varying orbital eccentricities. The integrations covered only 2000 orbit periods, so the extent displayed must be viewed as a lower limit.

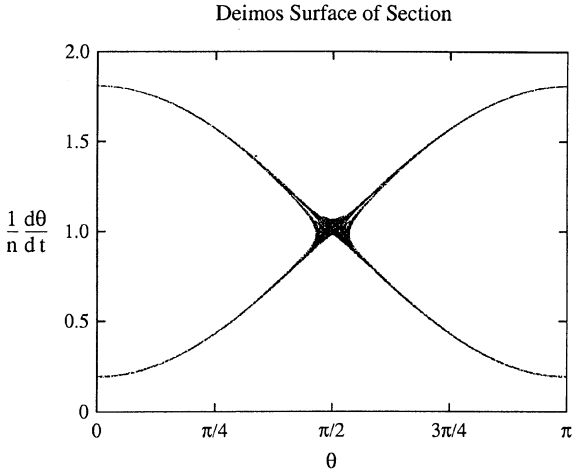

FIG. 3. The chaotic zone for Deimos ($\alpha = 0.81$) with its current eccentricity of 0.0005. Even with such a small eccentricity, the chaotic zone is not microscopic.

ity. Because of the limited nature of the integrations, the chaotic zone may extend significantly beyond the range plotted. For instance, with $e = 0.015$ the surface of section shows that the chaotic zone extends from roughly 0.65 to 1.25 near $\theta = \pi/2$, whereas in the more limited integration carried out for Fig. 2 the range is roughly 0.9–1.25. In any case, the chaotic zone is never microscopic. Phobos must have spent many hundreds of thousands, probably millions, of years in the chaotic zone.

The widths of the chaotic zones for several other irregularly shaped natural satellites are given in Table I. Considering the uncertainties in the orbital histories of the natural satellites, the current orbital eccentricity has been used in each calculation. It is plausible that this is representative of the eccentricity at the time of capture into synchronous rotation. Whether or not the eccentricity was near the current eccentricity, the widths in Table I illustrate that the chaotic zones for the irregularly shaped satellites are not negligibly small. Even for Deimos ($\alpha = 0.81$), where the eccentricity ($e \approx 0.0005$) is considered to be anomalously small (Yoder 1982), the chaotic zone cannot be ignored (Fig. 3). In fact, since the timescale for the tidal despinning of Deimos is on the order of 100 million years (Peale 1977), Deimos probably spent a considerably longer time in the chaotic zone than did Phobos.

III. ATTITUDE INSTABILITY

One of the most surprising facts about the rotational dynamics of Hyperion is that the synchronous spin-orbit resonance is attitude unstable (Wisdom *et al.* 1984). The spin axis cannot maintain an orientation perpendicular to the orbit plane. This is also true of the chaotic zone; the slightest deviation of the spin axis from the orbit normal leads to chaotic tumbling. The chaotic tumbling of Hyperion is a natural outcome of tidal evolution. Over the age of the solar system the spin axis is brought perpendicular to the orbit plane by the tidal torque as the spin is slowed toward synchronous rotation. Upon entering the chaotic zone, the slightest deviation of the spin axis from the equilibrium position leads to chaotic tumbling. Such a deviation will always exist due to the numerous minor perturbations to which Hyperion's obliquity is subject. It is natural to ask then whether the more narrow chaotic zones for other irregularly shaped natural satellites are attitude stable or not, and, if not, what is the range of the resulting out-of-plane motion.

Attitude stability of the chaotic zone may be defined in terms of Lyapunov Characteristic Exponents (LCEs) (Wisdom *et al.* 1984). The LCEs measure the mean exponential rate of divergence of nearby orbits. For chaotic orbits the distance between trajectories started sufficiently close to one another will, on the average, grow exponentially with time. The separation of nearby quasiperiodic orbits grows linearly, on the average. For a particular reference trajectory, the rate of exponential divergence can depend on the direction chosen to the neighboring trajectory. For an n degree of freedom problem there can, in general, be n distinct rates of exponential growth. There are n independent nonnegative LCEs. If the Hamiltonian contains no explicit time dependence, one of these must be zero, which corresponds to the neighboring trajectory being displaced along the direction of motion. For the time-dependent spin-orbit problem with the spin axis taking arbitrary orientations, there are three degrees of freedom with no integrals. Three LCEs may then be positive. LCEs may also be used to determine the attitude stability of motion in the fixed-axis chaotic zone. For rotation in the chaotic zone with the spin axis of the reference trajectory fixed perpendicular to the orbit plane, at least one of the Lyapunov exponents must be positive to reflect the chaotic nature of the reference trajectory. The chaotic zone is attitude unstable if two or more LCEs are positive. The use of LCEs to define attitude stability of a nonperiodic orbit is a natural generalization of the usual linear stability analysis for fixed points or Floquet analysis for periodic orbits where motion along the unstable eigendirection grows exponentially. In any case, the result of the analysis may be directly verified by computing a trajectory with spin axis slightly displaced from the orbit normal.

The remarkable result is that in every case studied the chaotic zone is attitude unstable, just as it is for Hyperion. Even more remarkable is that in every case the e-folding time for the growth of deviations of the spin axis from the orbit normal is small, on the order of 5–6 orbit periods! This is true even for Deimos with its small orbital eccentricity.

© American Astronomical Society • Provided by the NASA Astrophysics Data System

1987AJ.....94.1350W

A sample of the resulting tumbling motion for Phobos is depicted in Figs. 4 and 5. The angular coordinates used to represent the orientation of the body are slightly different from those used in Wisdom *et al.* (1984). Let a, b, and c denote a right-handed set of principal axes with the principal moments $A < B < C$, respectively. For a triaxial ellipsoid, a is aligned with the longest axis of the body. The orientation is specified relative to an inertial set of axes defined at periapse, with the x axis parallel to the planet-to-satellite line pointing away from the planet, the y axis in the direction of the orbital motion at periapse, and the z axis perpendicular to the orbit plane completing the right-handed set. Initially, the abc axes coincide with the xyz axes. Successive rotations of the abc set by the angle θ about the c axis, the angle ϕ about the new b axis, and then the angle $-\psi$ about the new a axis bring the principal axes to their actual orientation. When ϕ and ψ are zero, the angle θ is the same as the angle θ used to describe the orientation in the fixed spin-axis case. In this case, angle $\theta - f$ is the angle between the planet–satellite center line and the axis of smallest principal moment of inertia (the longest axis for a triaxial ellipsoid). For small eccentricities, $\theta - f \approx \theta - nt$. With this choice of angles, ϕ directly measures the angle of the axis of smallest moment of inertia (the long axis) from the orbit plane; this physically important angle is a more complicated function of the orientation angles in the original angular coordinates of Wisdom *et al.* (1984). Finally, the angle ψ measures the angle of rotation about the smallest moment of inertia (the long axis). The equations of motion are similar to those described in Wisdom *et al.* (1984). The trajectory plotted in Figs. 4 and 5 was started with the axis displaced 10^{-4} radians from the orbit normal, at the center of the attitude unstable 1/2 island. For Phobos the synchronous and 3/2 spin-orbit resonances are verified to be attitude stable, while the 1/2 resonance is attitude unstable. Points are plotted 100 times per orbit, for a total of 75 orbit periods. The resulting tumbling motion covers all values of ψ, but ϕ seems to have a limited range (Fig. 4). The maximum extent of the variation of $|\phi|$ over longer integrations of 200 orbit periods for Phobos as well as the other irregularly shaped satellites is given in Table I. Figure 5 shows that there is a tendency for the long axis to point towards the planet, but that at irregular intervals the long axis rotates by a π and the other end of the satellite points toward the planet.

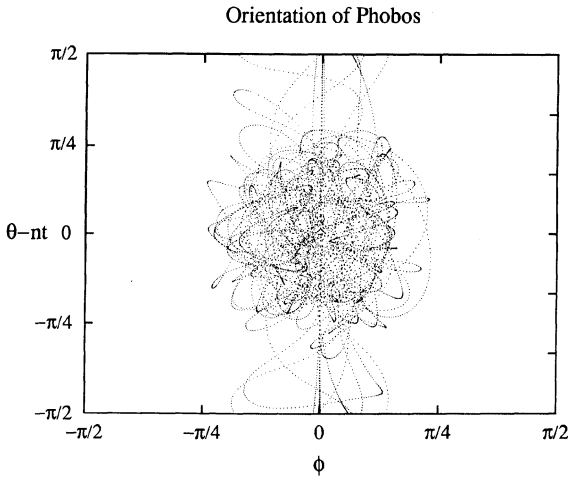

FIG. 5. The orientation of Phobos for 75 orbit periods. There is a tendency for the long axis to point toward Mars, but at irregular intervals the long axis reverses its orientation by 180°.

This tumbling motion is fully chaotic. The results of the calculation of the LCEs are displayed in Fig. 6. The LCEs are the asymptotic values of the quantity $\gamma = \ln[d(t)/d(t_0)]/(t - t_0)$ and measure the rates of exponential separation of nearby orbits (see Wisdom *et al.* 1984). The fact that three LCEs are positive indicates that there are no hidden integrals.

IV. TUMBLING PHASE SPACE

With the spin axis fixed perpendicular to the orbit plane, there is no chaotic behavior when the eccentricity is zero. Thus, the strong nature of the attitude instability for Deimos in its narrow chaotic zone is especially surprising. Since the eccentricity is so small ($e \approx 0.0005$), it cannot be responsible for the chaotic-tumbling motion. This argument is strengthened by the fact that the extent of the out-of-plane motion is relatively insensitive to the principal moments and orbital

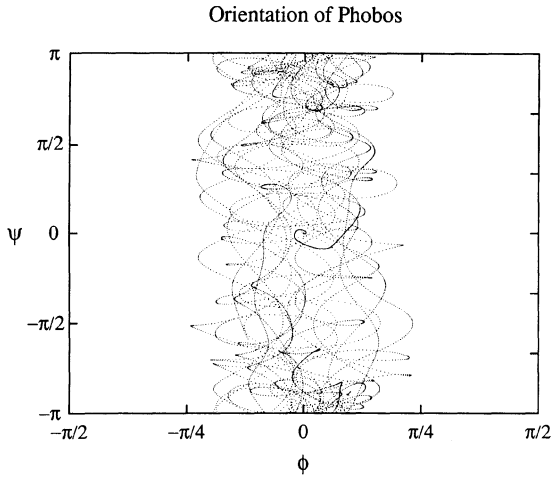

FIG. 4. The orientation of Phobos for 75 orbit periods. The long axis can deviate by as much as 1.29 radians from the orbit plane, while rotation about the long axis is complete.

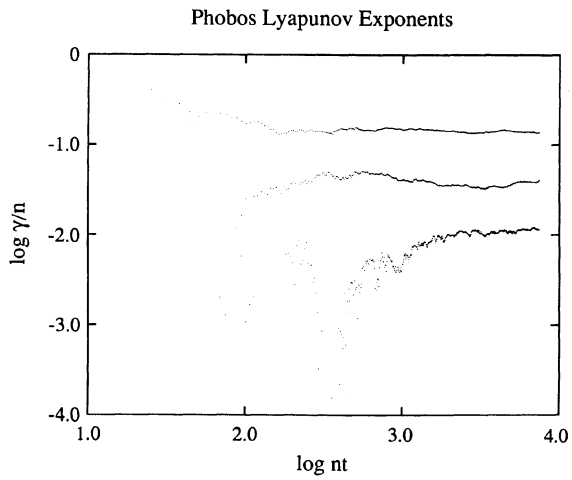

FIG. 6. Calculations of the Lyapunov Characteristic Exponents for the chaotic-tumbling motion of Phobos. The LCEs are the limiting values of γ for large t.

© American Astronomical Society • Provided by the NASA Astrophysics Data System

1987AJ.....94.1350W

eccentricity of the natural satellites (see Table I). Of course, the eccentricity does have a strong effect on the dynamics; it is almost certainly the case that the extent of the chaotic zone is always greater for a larger eccentricity. For instance, for Hyperion, where the shape is similar to Phobos but the orbital eccentricity is an order of magnitude larger, the angle ϕ goes through all values. However, if the eccentricity is small and there are still significant chaotic variations in the angles, the chaotic behavior must be purely a consequence of the gravity gradient torque on the out-of-round satellite. The existence of a large out-of-the-plane chaotic zone with *zero* orbital eccentricity has been confirmed numerically.

To some extent this should have been expected. Integrable problems generally lose the full complement of integrals upon perturbation (Poincaré 1892). While the free motion of a rigid body is integrable, the motion of a rigid body subject to a gravity gradient torque is expected on general grounds to be nonintegrable. In fact, while there is an analytic integral of the motion when the orbit is circular analogous to the Jacobi integral for the (circular) restricted three-body problem (which is the Hamiltonian in the rotating frame), there are still three degrees of freedom. Only two are required for chaotic behavior.

Perhaps some insight into this chaotic-tumbling motion can be achieved by reducing the problem still further. If, besides taking the orbit to be circular, the two largest principal moments are taken to be equal, i.e., $B = C$, then the Hamiltonian is cyclic in ψ, the angle of rotation about the axis of smallest principal moment of inertia. Consequently, the momentum conjugate to ψ, the component of the angular momentum along the principal axis of smallest principal moment of inertia, is conserved. There is thus another integral of the motion, which is clearly independent of the "Jacobi integral," and the problem is reducible to two degrees of freedom. It is then possible to make surfaces of section for the three-dimensional tumbling motion. Examination of Fig. 5 shows that the angle $\theta - nt$ frequently goes through zero, whether or not the long axis is librating. This suggests that a good choice for the surface of section is to plot the momentum conjugate to ϕ vs ϕ, whenever $\theta - nt$ goes through 0. When $B = C$, the momentum conjugate to ϕ is simply proportional to $d\phi/dt$, which is what has actually been plotted. There is one complication in the computation of the surface of section. In many examples, the Hamiltonian is quadratic in the momentum conjugate to the section variable. Resolving the ambiguity of which crossings to plot is then easy: only those with one particular sign of the momentum are displayed. With such a choice, each point on the surface of section corresponds to a unique trajectory. In the case at hand, the Hamiltonian is not quadratic in p_θ, so an alternate prescription must be made. The prescription chosen is the following. Given the value of the integrals of the motion and the coordinates of the point on the section, the possible values of p_θ are solutions of a quadratic equation. If the p_θ corresponds to the largest of the two roots of the quadratic equation, the point is plotted. This is a natural generalization of the usual section for Hamiltonians that are quadratic in the momenta.

The surface of section for a Phobos-like prolate ellipsoid is shown in Fig. 7. Here $A/C = 0.6538$, and $B = C$. The integral p_ψ and the "Jacobi integral" have values appropriate for motion that is intially just at the synchronous separatrix, with no rotation about the long axis; this is the configuration expected of a natural satellite just before capture. The outermost curve is the limit imposed by the integrals. The surface of section has a number of interesting features. First is the fact that a large chaotic zone even exists. Next, note that the chaotic zone extends to $\phi = 0$. Even in the zero-eccentricity case, at the point of capture into synchronous rotation the spin axis is attitude unstable! It is also interesting to note that there are quasiperiodic islands at large displacements of the long axis from the orbit plane. An examination of the trajectories, though, reveals that these islands are special cases of synchronous rotation. The long axis never makes a complete rotation by π relative to the planet. This is also true of the chaotic zone for these values of the integrals. If, on the other hand, the surface of section is computed for a somewhat larger "Jacobi integral" for which the angle $\theta - nt$ circulates when ϕ is near zero, the chaotic zone still exists but no longer extends all the way to the origin. Away from the synchronous resonance, the motion near $\phi = 0$ is attitude stable. In this case, motion in the chaotic zone alternately librates and circulates.

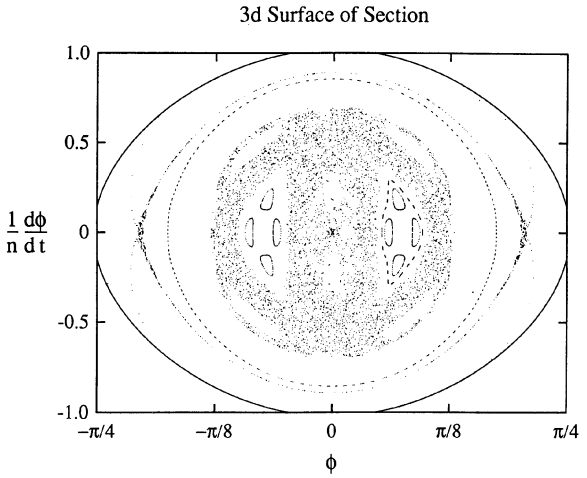

FIG. 7. Surface of section for the out-of-plane motion of a prolate, axisymmetric body in a circular orbit. The integrals are chosen to be those of a body just like the synchronous rotation separatrix, with no rotation about the long axis. The chaotic zone extends to the origin; even in this extreme case the spin axis perpendicular to the orbit plane is attitude unstable.

For completeness, when the eccentricity is zero, the Hamiltonian in the rotating frame (the "Jacobi integral") is

$$H = \tfrac{1}{2}(A\omega_a^2 + B\omega_b^2 + C\omega_c^2) + \tfrac{3}{2}(A\alpha^2 + B\beta^2 + C\gamma^2) - np_\theta , \quad (5)$$

where α, β, and γ are the direction cosines of the principal axes on the planet-to-satellite line, and ω_a, ω_b, and ω_c are the components of the rotation vector on the principal axes. For the case where $B = C$,

$$p_\theta = (A \sin^2\phi + C\cos^2\phi)\frac{d\theta}{dt} + A\sin\phi\frac{d\psi}{dt} . \quad (6)$$

The second integral is

$$p_\psi = A\left(\frac{d\theta}{dt}\sin\phi + \frac{d\psi}{dt}\right) . \quad (7)$$

In the numerical integrations, both integrals are typically conserved to about ten significant digits.

© American Astronomical Society • Provided by the NASA Astrophysics Data System

1987AJ.....94.1350W

V. ORBITAL EVOLUTION

Dissipation of energy in a tumbling satellite may have a significant effect on the orbital evolution of the satellite. This section presents some initial considerations on this problem.

In terms of the orbital energy E and orbital angular momentum L, the rate of change of the eccentricity of an orbit is

$$\frac{de}{dt} = -\frac{1-e^2}{2e}\left(\frac{2}{L}\frac{dL}{dt} + \frac{1}{E}\frac{dE}{dt}\right), \tag{8}$$

while the rate of change of the semimajor axis is

$$\frac{1}{a}\frac{da}{dt} = -\frac{1}{E}\frac{dE}{dt}. \tag{9}$$

Variations in the orbital energy and in the angular momentum will be discussed separately.

Energy is dissipated in the satellite as a result of the time-dependent solid-body tides raised on the satellite by the planet, and also by any bending the body undergoes as a result of the applied torques and nonprincipal axis rotation. For a synchronously rotating satellite, there is no time-dependent tide at all unless the orbit is eccentric; in synchronous rotation, the rate of energy dissipation is proportional to the square of the orbital eccentricity. In a tumbling or nonsynchronously rotating satellite, the whole magnitude of the tide is time dependent; the rate at which energy is dissipated in the satellite is significantly enhanced over that in a synchronous rotation, especially when the orbital eccentricity is small. The variation in the energy is always negative (it is dissipated), and in a steady state this energy must ultimately come from the orbital energy.

Before discussing the variation of the angular momentum, it is helpful to first introduce the notion of the rotational or dynamical "state" of a system. In this context, a rotational "state" will denote a dynamical state of the spin-orbit system distinguishable from other dynamical states by more than simple time translation. If there exists a trajectory that comes arbitrarily close to two particular points in the phase space, then those two points will be considered to belong to the same state. While motion in a chaotic zone has not been rigorously proven to be ergodic, in practice it appears to be so. Thus all points in a chaotic zone belong to the same dynamical state. Measure-zero sets of unstable periodic orbits are excluded from consideration. Quasiperiodic motion of an n degree of freedom system occurs on an n torus in the phase space, and is ergodic on that torus. Thus all points on that torus belong to the same dynamical state since for almost all initial conditions on the torus trajectories eventually come arbitrarily close to all other points on the torus. On the other hand, trajectories on different tori belong to different dynamical states, and so do trajectories in disjoint chaotic zones. Chaotic trajectories are necessarily in different dynamical states from quasiperiodic trajectories. If the dynamical system has explicit integrals of the motion, the state will be different if the integrals have different values. All trajectories in a system with one set of parameters are distinguishable from trajectories of the system with a different set of parameters; changing a parameter changes the state. The state thus indicates a component of the phase space that is ergodically indecomposable. One property of the dynamical state as just defined is that if the time average of some quantity computed along a trajectory in a particular state is well defined, then it may equally well be computed by an average over the set of points in the phase space that belong to that state, or alternatively, the time average of the quantity along two different trajectories belonging to the same state will be equal.

Since the total angular momentum is conserved, the angular momentum may only change its distribution among the components of the system. An increase in orbital angular momentum must be compensated by a decrease in the rotational angular momentum, and *vice versa*. The rotational angular momentum may be changed through the dynamical torque or the tidal torque. The dynamical torque gives rise to the various dynamical rotation states. In most rotation states the rotational angular momentum varies as the trajectory evolves, with the timescale for changes in the rotational angular momentum being on the order of the orbital period. Of course, changes in the rotational angular momentum are exactly compensated by changes in the orbital momentum. However, for a small-body near-synchronous rotation the angular momentum in the spin is very much smaller than the angular momentum in the orbit; the ratio being of the order of the square of the ratio of the radius of the satellite to the semimajor axis of the orbit. For example, for Deimos near-synchronous rotation, the ratio of spin angular momentum to orbital angular momentum is approximately 10^{-7}. Even a drastic modification of the rotation state produces a negligible change in the orbit. It is quite a good approximation to ignore the changes in the orbit in determining the short-term dynamical behavior. On the other hand, the timescale for changes in a dynamical state due to tidal friction is typically much longer than an orbital period, perhaps even millions of orbit periods. The details of the dynamical changes that occur on the orbital timescale must be irrelevant to the evolution that occurs on the tidal timescale. Evidently, the property of the dynamical state that is relevant to the long-term tidal evolution is just the average angular momentum, since changes in the average rotational angular momentum must reflect changes in the average orbital angular momentum. The reason for introducing the notion of state is just for the purpose of being able to talk about those factors that affect the average angular momentum. If the rotational angular momentum is a well-defined quantity for all rotational states, it is clear that different particular trajectories belonging to equivalent states should have the same average angular momentum, and that the average angular momentum can only change through a change in the dynamical state of the system. By definition, the state does not change through the normal dynamical evolution of the system due to dynamical torques, but can only change through the external action of the tidal torque. Only the tidal torque can change the average angular momentum. For this approach to be useful in the consideration of the tidal evolution of the orbit, the timescale for a well-defined average to be established must be shorter than the timescale for tidal evolution. It is a reasonable expectation that this should be the case, but this point is discussed further below.

The rotational state, and consequently the average angular momentum of the state, depends only on the orbital eccentricity and semimajor axis, the two independent ratios of the principal moments of inertia of the satellite, and the initial conditions, although many initial conditions may correspond to the same state. The ratios of principal moments will be considered as given in this problem, and their dependence on the state will not be further considered. The dependence of the average angular momentum on the semimajor axis can be explicitly given since the semimajor axis enters only through the orbital mean motion, which in turn only determines the dynamical timescale (see Eq. (1)). Let the average

© American Astronomical Society • Provided by the NASA Astrophysics Data System

1987AJ.....94.1350W

angular momentum perpendicular to the orbit plane be denoted $\langle L_z \rangle$, where the angular brackets indicate time average. It is convenient to also introduce the dimensionless average angular momentum perpendicular to the orbit plane $\mathscr{L}_z = \langle L_z \rangle / Cn$, where n is the orbital mean motion and C is the largest moment of inertia. The dimensionless average angular momentum does not depend on the semimajor axis.

As an illustration, consider the evolution of the orbit while the rotation is locked in the synchronous spin-orbit resonance. For all states that are locked in synchronous rotation about the largest principal moment of inertia, the dimensionless average angular momentum is $\mathscr{L}_z = 1$, independent of the amplitude of libration. The average angular momentum does not depend on the eccentricity and depends only trivially on the semimajor axis. As long as the rotation remains locked in synchronous rotation, the dimensionless angular momentum cannot change. Thus

$$\frac{d\langle L_z \rangle}{dt} = \mathscr{L}_z C \frac{dn}{dt} = C \frac{dn}{dt}. \tag{10}$$

The rate of change of the average orbital angular momentum is exactly opposite:

$$\frac{d\langle L_{\rm orbit} \rangle}{dt} = -\frac{d\langle L_z \rangle}{dt} = -C \frac{dn}{dt}. \tag{11}$$

This can be rewritten

$$\frac{1}{\langle L_{\rm orbit} \rangle} \frac{d\langle L_{\rm orbit} \rangle}{dt} = -\frac{L_z}{\langle L_{\rm orbit} \rangle} \frac{1}{n} \frac{dn}{dt}$$

$$= -\frac{\langle L_z \rangle}{\langle L_{\rm orbit} \rangle} \frac{3}{2E} \frac{dE}{dt}. \tag{12}$$

The rate at which e changes due to tidal dissipation is then, by Eq. (8),

$$\frac{de}{dt} = -\frac{1-e^2}{2e} \left(1 - \frac{3\langle L_z \rangle}{\langle L_{\rm orbit} \rangle}\right) \frac{1}{E} \frac{dE}{dt}. \tag{13}$$

Since the spin angular momentum is miniscule compared to the orbital angular momentum, the standard result (Goldreich 1963) is recovered.

The real concern here is with the determination of the orbital variations due to the enhanced dissipation of energy in a chaotic-tumbling state. In the case of chaotic tumbling, the dimensionless average angular momentum depends on the orbital eccentricity, and in the case of zero orbital eccentricity, on the initial conditions as well. However, when the orbital eccentricity is nonzero, motion in the chaotic zone near synchronous rotation does not possess any integrals of the motion since the three Lyapunov exponents are all positive (Sec. III). Thus, in this case, there can be no dependence of the average angular momentum on initial conditions, as long as the trajectory is in the large chaotic zone. Consequently, the dimensionless average angular momentum depends only on the orbital eccentricity, $\mathscr{L}_z = \mathscr{L}_z(e)$. The average angular momentum depends on the orbital eccentricity because the extent of the chaotic zone depends on the eccentricity. Once this function is known, the effect of tidal dissipation on the orbit can be calculated just as was done for rotation in the synchronous resonance above. Namely, the secular rate of change of the spin angular momentum is

$$\frac{d\langle L_z \rangle}{dt} = \mathscr{L}_z C \frac{dn}{dt} + Cn \frac{d\mathscr{L}_z}{de} \frac{de}{dt}. \tag{14}$$

Dividing through by $\langle L_z \rangle$,

$$\frac{1}{\langle L_z \rangle} \frac{d\langle L_z \rangle}{dt} = \frac{1}{n} \frac{dn}{dt} + \frac{1}{\mathscr{L}_z} \frac{d\mathscr{L}_z}{de} \frac{de}{dt}. \tag{15}$$

Thus,

$$\frac{1}{\langle L_{\rm orbit} \rangle} \frac{d\langle L_{\rm orbit} \rangle}{dt}$$

$$= -\frac{\langle L_z \rangle}{\langle L_{\rm orbit} \rangle} \left(\frac{1}{n} \frac{dn}{dt} + \frac{1}{\mathscr{L}_z} \frac{d\mathscr{L}_z}{de} \frac{de}{dt} \right). \tag{16}$$

Substituting into Eq. (8) and rearranging yields

$$\frac{de}{dt} = \left[-\frac{1-e^2}{2e} \left(1 - \frac{3\langle L_z \rangle}{\langle L_{\rm orbit} \rangle}\right) \frac{1}{E} \frac{dE}{dt} \right] \Bigg/ \left(1 - \frac{1-e^2}{e} \frac{\langle L_z \rangle}{\langle L_{\rm orbit} \rangle} \frac{1}{\mathscr{L}_z} \frac{d\mathscr{L}_z}{de}\right). \tag{17}$$

The factor involving $\langle L_z \rangle / \langle L_{\rm orbit} \rangle$ in the numerator is ignorable. The analogous factor in the denominator is important if the quantity

$$\frac{1}{e} \frac{\langle L_z \rangle}{\langle L_{\rm orbit} \rangle} \frac{1}{\mathscr{L}_z} \frac{d\mathscr{L}_z}{de}$$

has a magnitude of order unity or greater. For Deimos, say, where $e = 0.0005$ and $\langle L_z \rangle / \langle L_{\rm orbit} \rangle \approx 10^{-7}$, the factor is important if $d\mathscr{L}_z/de$ exceeds about 5000. Unfortunately there appears to be no other way to determine $\mathscr{L}_z(e)$ other than by numerical computation.

Considerable effort (about 500 VAX hr) has been expended in an attempt to estimate $\mathscr{L}_z(e)$ for the principal moments estimated from the shape of Deimos. The results are shown in Fig. 8. For each eccentricity three trajectories in the chaotic zone surrounding the synchronous resonance were integrated for 5000 orbit periods each. The diamonds indicate the average angular momentum perpendicular to the orbit plane for each eccentricity. The error bars indicate an estimate of the error of these averages. The error estimate has a contribution from the standard deviation of the mean of each individual trajectory which is determined by consid-

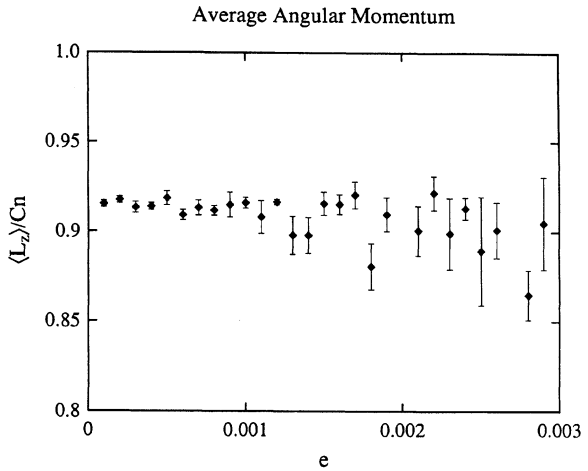

FIG. 8. Estimates for Deimos of the dimensionless average angular momentum perpendicular to the orbit plane, $\mathscr{L}_z = \langle \mathscr{L}_z \rangle / Cn$, as a function of the orbital eccentricity, e.

© American Astronomical Society • Provided by the NASA Astrophysics Data System

1987AJ.....94.1350W

ering each 500 orbit-period segment as a separate experiment and a contribution from the standard deviation of the mean of the means of the three separate trajectories. The average angular momentum was unexpectedly difficult to determine. The averages shown in Fig. 8 are rather noisy and are only marginally consistent with a smooth curve running through them. Apparently, integrations much longer than 5000 orbit periods are required to obtain consistent averages of the angular momentum. The difficulty probably arises because any particular trajectory may spend considerable time in small tributaries of the chaotic zone, spoiling the average in any limited integration. This problem is particularly acute in the full three-dimensional tumbling problem since the interconnectedness of the chaotic zone in many dimensions (the "Arnold web") can allow the trajectory to wander far from the primary chaotic zone. While in the reduced spin-orbit problem with one and one-half degrees of freedom the chaotic zone is limited in extent, and there is little doubt that the angular momentum has a well-defined average, it is not clear that such an average is mathematically well defined in the three-dimensional problem. If the average is not well defined, then the outcome of tidal evolution will depend on which particular part of the Arnold web the trajectory explores on the tidal-evolution timescale, and the considerations in this section will not be applicable. However, even in that case the estimates in this section will apply to those periods when the rotation trajectory is in the main chaotic zone near synchronous rotation. The data presented in Fig. 8 represent the best estimate available of the function $\mathscr{L}_z(e)$. There is no convincing evidence in these data that $d\mathscr{L}_z/de$ is greater than about 100. Thus taking the data in Fig. 8 at face value, the denominator in Eq. (17) may be neglected. The resulting rate of decrease of the orbital eccentricity while the rotation is in the chaotic-tumbling state then takes the same form as for synchronous rotation

$$\frac{de}{dt} = -\frac{1-e^2}{2e}\frac{1}{E}\frac{dE}{dt}. \tag{18}$$

Energy dissipation results from the nonperiodic solid-body tides raised by the planet, and the deformation induced by the chaotic tumbling itself. Dissipation of energy in a tumbling satellite is significantly enhanced over that in a synchronously rotating satellite since the whole magnitude of the tide is time dependent for a nonsynchronous rotation. For a chaotically tumbling satellite, the rate of energy dissipation must be comparable to and is probably somewhat greater than that in a nonsynchronous satellite with a regular rotation. The order of magnitude of the energy dissipated per orbit period is

$$\Delta E \approx \rho^2 \omega^4 R^7/\mu Q, \tag{19}$$

where ρ is the mass density, ω is the rotational angular velocity, R is the radius of the satellite, Q is the specific dissipation function, and μ is the shear modulus (Burns and Safronov 1973). Q is of order 100, and μ is of order 10^{12} dyn/cm^2. For the chaotic-tumbling state, ω is within a factor of 2 of the orbital mean motion n. Shape parameters and "nutation" angles are all of order unity, and have been neglected. Thus the eccentricity of a chaotically tumbling satellite is damped at a rate of order

$$\frac{1}{e}\frac{de}{dt} \approx -\frac{\rho n^3 R^4}{e^2 \mu Q a^2}. \tag{20}$$

This damping rate should not be taken too literally since numerical coefficients have been consistently ignored in its derivation. The important point is that the timescale for the damping of eccentricity is two factors of e smaller for a chaotically tumbling satellite than for a synchronously rotating satellite.

This picture of the orbital evolution for a chaotically tumbling satellite may be contrasted with the orbital evolution of a nonsynchronously rotating satellite. For a nonsynchronously rotating satellite, both the orbital energy and angular momentum are modified by the tidal torques. In this case the predicted outcome will depend on the tidal model, since $dL/dt < 0$ and $dE/dt < 0$ with $E < 0$ are competing effects. Generally, for rapid rotation the orbital eccentricity increases, but de/dt may change sign as synchronous rotation is approached, depending on the tidal model.

There are two possibilities for the ultimate outcome of the tidal evolution of a satellite in chaotic rotation. First, the rotation trajectory may "stick" to some quasiperiodic island in the phase space long enough that the rotation is captured into the quasiperiodic island by the weak tidal torques. Such "sticking" is a well-known feature of the motion in a chaotic zone. Since the synchronous state dominates the phase space when the eccentricity is small, it is the most likely final state (presuming it is attitude stable). Alternatively, the rotation may remain chaotic until the eccentricity has damped to zero. Once the eccentricity is zero, further evolution depends on variations of the "Jacobi integral." It seems likely that the Jacobi integral will be damped at a rate comparable to the rate at which the rotational energy is damped, since the Jacobi integral is equal to the rotational energy minus the mean motion times the rotational angular momentum. Denoting the "Jacobi integral" by J, the damping rate is of order

$$\frac{1}{J}\frac{dJ}{dt} \approx -\frac{\rho n^3 R^2}{\mu Q}, \tag{21}$$

where Eq. (19) has again been used for the rate of dissipation of rotational energy and the rotational energy has been taken to be of order Cn^2. The change in the Jacobi integral needed to significantly reduce the chaotic zoner is presumably less than the difference in the Jacobi integral at the separatrix and the Jacobi integral of damped synchronous libration, which is of order Cn^2. Comparing the two damping rates, Eqs. (20) and (21), the latter is larger by a factor a^2e^2/R^2, where the eccentricity to be used is that used in calculating the eccentricity damping rate. Thus if the chaotic tumbling did persist to the point of completely damping the eccentricity, the chaotic tumbling would then be damped at a somewhat faster rate through the secular damping of the rotational "Jacobi integral," J.

In summary, the rotational tumbling motion in the large chaotic zone near synchronous rotation leads to a rapid damping of the orbital eccentricity on the timescale roughly given by Eq. (20), which is two factors of the orbital eccentricity shorter than the timescale for damping the eccentricity while in synchronous rotation.

VI. DISCUSSION

The chaotic tumbling of Hyperion is no longer just an isolated curiosity. Rather, chaotic tumbling is a natural and inevitable stage in the rotation histories of all the irregularly shaped natural satellites, regardless of their orbital eccentricity. The large eccentricity of Hyperion's orbit simply exacerbates the chaotic tumbling which would have occurred in any case. The regular progression of the spin axis driven to the orbit normal by the tidal torque, while the spin slows and

© American Astronomical Society • Provided by the NASA Astrophysics Data System

1987AJ.....94.1350W

is ultimately captured into the final synchronous rotation state, is now see to be interrupted by the birth pangs of a period of chaotic tumbling. Ultimately, chaotically tumbling satellites are captured into a state that is stable to further tidal dissipation, which in every case observed is the synchronous state. Even if other states are stable, with such small eccentricities the synchronous state is by far the largest quasiperiodic island and could consequently be expected to be the most probable endpoint. Hyperion is still in the chaotic zone today because the despinning timescale is so long and the synchronous state is attitude unstable for Hyperion. Unfortunately, it is not yet possible to estimate the capture probability or the time spent in the chaotic zone. Simulations for Hyperion indicated that trajectories often spend much more time in the chaotic zone than they would if that part of the phase space had been regular. Qualitatively, motion in the chaotic zone is so irregular that the weak tidal torque cannot make any secular progress. Capture from the chaotic zone instead relies on the trajectory being temporarily stuck to the border for a long enough time that the tidal torque can remove it from the chaotic zone (Wisdom *et al.* 1984).

The new understanding of the rotation histories of the irregularly shaped natural satellites is interesting and important in itself; the world works in a surprising way. Nevertheless, are there any directly observable consequences of this episode of chaotic tumbling for the irregularly shaped satellites? Several possibilities come to mind. The first is Miranda. Is it possible that its exotic surface features are a result of a period of chaotic tumbling? This appears unlikely. While the enhanced tidal dissipation during a period of chaotic tumbling could have provided a significant heat source, the attitude instability described above occurs only as the synchronous rotation state is entered. For Miranda this must have occurred soon after its formation, since the timescale for tidal despinning to synchronous rotation is only 300 000 yr (Peale 1977). Thus the episode of chaotic tumbling associated with the entry into synchronous rotation would have occurred too close to the time of formation to account for the disparate ages of the features seen on Miranda.

The surface of Phobos is marked by a series of linear grooves. A number of possible causes for these grooves have been suggested. Soter and Harris (1977) suggested the grooves were caused by increasing tidal stresses as the orbit of Phobos decays. This would imply that the grooves are young. However, subsequent examination of the number of craters superimposed on the grooves indicated that the grooves are old (greater than 10^9 yr). Thomas *et al.* (1978) suggested that since the grooves are most prominent near the largest crater, Stickney, they may be a result of the event that created that crater. Weidenshilling (1979) objects that the grooves bear no simple relationship to the crater, and claims that since some of the grooves show cross cutting the grooves did not form simultaneously. Weidenshilling proposes instead that the event that created Stickney broke the previously established synchronous rotation lock, and the tidal stresses from the subsequent "nutation" caused the faulting along planes of maximum shear stress, producing the system of grooves. In this scenario, more grooves appear near Stickney because the material was weakened by the impact. The study reported in this paper has now established that chaotic tumbling is a natural part of the rotation history of Phobos, whatever eccentricity Phobos had at the time of capture into synchronous rotation. If a nutation that would result from an impact is capable of creating the grooves, then certainly the chaotic tumbling that Phobos underwent as it entered synchronous rotation could have done the same. Still, Stickney must have already been present when the grooves were formed since there must be some reason for the association of the grooves with the crater. Another possibility, following Weidenshilling, is that the impact that created Stickney drove Phobos into the chaotic zone and the stresses from the resulting chaotic tumbling created the grooves. Displacing the long axis from the orbit plane by 20° can initiate chaotic tumbling. This places an upper limit on the amplitude of a regular "nutation" in synchronous rotation (however, see Sec. IV). The impact hypothesis of Thomas *et al.* is still the simplest explanation for the grooves on Phobos.

If the grooves on Phobos were a result of a period of chaotic tumbling as the synchronous state was entered, then there may be grooves on other irregularly shaped satellites since they have all experienced a period of chaotic tumbling. Does the lack of grooves on Deimos then rule out the possibility that the grooves on Phobos were created by chaotic tumbling? Tidal stresses arise from the gravitational potential of Mars as well as the centrifugal potential of the chaotic rotation itself. Using Kelvin's formula for the displacement Love number and recalling that the rate of rotation of a chaotically tumbling body is of the same order as the orbital mean motion, the tidal stresses are all proportional to $R^2 a^{-3}$, where R is the radius of the satellite and a is the semimajor axis. Deimos is smaller than Phobos and farther from Mars. Currently, the ratio of the semimajor axes is 2.5, but all orbital histories of Phobos and Deimos place the satellites closer to one another in the past since the corotation radius lies between them. The grooves on Phobos are at least 10^9 yr old, most orbital histories would then place Phobos beyond 4 Martian radii, where the ratio of semimajor axes must have been less than 2. Deimos is roughly half the size of Phobos. The tidal stresses would then have differed by a factor in the neighborhood of 30. Perhaps this difference in tidal stress could account for the absence of grooves on Deimos. Perhaps it is necessary to appeal again to weaknesses induced by the event that created Stickney. In this case it is not possible to make predictions regarding grooves on other satellites. Perhaps the grooves are simply unrelated to the episode of chaotic tumbling.

Another possible consequence of the chaotic tumbling of irregularly shaped satellites concerns the eccentricity of Deimos. Yoder (1982) has shown that passage through a variety of resonances could completely account for the eccentricity of Phobos, even assuming a zero initial eccentricity before the resonance encounters. Similar analysis shows that Deimos should have an eccentricity of order 0.002, from passage through a 2/1 mean motion resonance with Phobos on the order of two billion years ago. Instead, the eccentricity of Deimos is less than 0.0005. Dissipation of energy within a satellite tends to decrease the orbital eccentricity if the rotation is locked in synchronous rotation (Urey *et al.* 1959; Goldreich 1963), but the timescale for the damping of the eccentricity of Deimos is much greater than the age of the solar system. Yoder concluded that either the orbit was circularized by an exceptional impact which occurred just before resonance encounter, or there has been significantly larger tidal dissipation in Deimos than in Phobos. The small orbital eccentricity of Deimos could also be a consequence of an episode of chaotic tumbling.

Evaluating expression (19) for Deimos using an eccen-

© American Astronomical Society • Provided by the NASA Astrophysics Data System

1987AJ....94.1350W

tricity of 0.002 gives a timescale of 300 million years. Now the timescale for Deimos to reach synchronous rotation is of order 100 million years (Peale 1977). It is thus possible that Deimos could spend enough time in the chaotic zone to damp out an initial eccentricity of 0.002. Yoder estimated that the resonance was encountered about two billion years ago, but there is considerable uncertainty in this estimate (personal communication, Yoder 1986). Consequently, it is difficult to say whether the rotation is likely to have been chaotic after the resonance passage, but it is certainly possible. Perhaps the resonance passage occurred much earlier when Deimos was more likely to still be chaotically tumbling. The evolution of the eccentricity of Deimos deserves further attention.

The timescale for damping the eccentricity of Phobos is about five million years, using an initial eccentricity of 0.02. This is to be compared with the timescale to reach synchronous rotation of a few million years. Whether or not the dissipation resulting from the chaotic tumbling can explain the observed low eccentricity of Deimos after passage through resonance, it may help account for the initial circularization of the orbits of both Phobos and Deimos.

For Hyperion, with an eccentricity of 0.1, Eq. (10) yields a timescale much greater than the age of the solar system. Apparently, the dissipation in Hyperion has a negligible effect on its orbital evolution. It cannot be used to solve the timescale problem for the establishment of the 4/3 Titan-Hyperion mean-motion commensurability.

VII. SUMMARY

The rotation histories of the irregularly shaped satellites differ significantly from the standard picture of tidal evolution of satellite rotations. Just before capture into the synchronous rotation resonance a narrow, but not microscopic, chaotic zone is entered. This chaotic zone is attitude unstable, and the satellite begins to tumble chaotically. For those natural satellites with α of order unity and small eccentricity, the long axis deviates from the orbital plane by angle of order 1 radian during the chaotic-tumbling motion, while complete rotations about the long axis are made. Enhanced dissipation of energy during the chaotic-tumbling phase may have a significant effect on the orbital evolution, and the possibility of chaotic tumbling must certainly be kept in mind in determining the orbital histories of irregularly shaped natural satellites. Eventually, the rotation stays close to one of the accessible attitude-stable islands long enough for the weak tidal torque to remove the satellite from the chaotic zone. The rotation histories of irregularly shaped satellites are considerably more complicated than previously thought.

I would like to thank S. J. Peale and W. Tittemore for helpful conversations. This research was supported in part by the NASA Planetary Geology and Geophysics Program under grant NAGW-706.

REFERENCES

Binzel, R. P., Green, J. R., and Opal, C. B. (1986). Nature **320**, 511.
Burns, J. A., and Safronov, V. S. (1973). Mon. Not. R. Astron. Soc. **165**, 403.
Cazenave, A., Dobrovolskis, A., and Lago, B. (1981). Icarus **44**, 730.
Chirikov, B. V. (1979). Phys. Rep. **52**, 263.
Darwin, G. (1879). Philos. Trans. Part I.
Duxbury, T. C., and Callahan, J. D.(1982). Lunar Planet. Abst. **13**, 190.
Goguen, J. (1983). Paper presented at IAU Colloquium No. 77, Natural Satellites, Ithaca, NY, July 5–9.
Goldreich, P. (1963). Mon. Not. R. Astron. Soc. **126**, 257.
Goldreich, P., and Peale, S. J. (1966). Astron. J. **71**, 425.
Goldreich, P., and Peale, S. J. (1970). Annu. Rev. Astron. Astrophys. **6**, 287.
Hénon, M., and Heiles, C. (1964). Astron. J. **69**, 73.
Lambeck, K. (1979). J. Geophys. Res. **84**, 5651.
Mignard, F. (1981). Mon. Not. R. Astron. Soc. **194**, 365.
Peale, S. J. (1977). In *Planetary Satellites*, edited by J. Burns (University of Arizona, Tucson), pp. 87-112.
Pettengill, G. H., and Dyce, R. B. (1965). Nature **206**, 1240.
Poincaré, H. (1892). *Les Méthodes Nouvelles de la Méchanique Céleste* (Gauthier-Villars, Paris).
Singer, S. F. (1968). Geophys. J. **15**, 205.
Soter, S., and Harris, A. (1977). Nature **268**, 421.
Smith, B., *et al.* (1982). Science **215**, 504.
Thomas, P., Veverka, J., and Duxbury, T. (1978). Nature **273**, 282.
Thomas, P., *et al.* (1984). Nature **307**, 716.
Thomas, P., and Veverka, J. (1985). Icarus **64**, 414.
Urey, H. C., Elsasser, W. M., and Rochester, M. G. (1959). Astrophys. J. **129**, 842.
Weidenshilling, S. (1979). Nature **282**, 697.
Wisdom, J., Peale, S. J., and Mignard, F. (1984). Icarus **58**, 137.
Yoder, C. F. (1982). Icarus **49**, 327.

© American Astronomical Society • Provided by the NASA Astrophysics Data System